DOI 10.5012/bkcs.2011.32.7.2358

Theoretical Studies on Electronic Structure and Absorption Spectrum of Prototypical Technetium-Diphosphonate Complex ^{99m}Tc-MDP

Ling Qiu,[*] Jian-Guo Lin,[*] Xue-Dong Gong,[†] Xue-Hai Ju,[†] and Shi-Neng Luo

Key Laboratory of Nuclear Medicine, Ministry of Health, Jiangsu Key Laboratory of Molecular Nuclear Medicine, Jiangsu Institute of Nuclear Medicine, Wuxi 214063, P. R. China. [*]E-mail: qiulingwx@gmail.com(L.Q.), jglin@yahoo.cn(J.-G. L.)
[†]Institute for Computation in Molecular and Material Science, School of Chemical Engineering, Nanjing University of Science and Technology, Nanjing 210094, P. R. China
Received February 2, 2011, Accepted May 30, 2011

Density functional theory (DFT) and time-dependent density functional theory (TDDFT) calculations, employing the B3LYP method and the LANL2DZ, 6-31G*(LANL2DZ for Tc), 6-31G*(cc-pVDZ-pp for Tc) and DGDZVP basis sets, have been performed to investigate the electronic structures and absorption spectra of the technetium-99m-labeled methylenediphosphonate (^{99m}Tc-MDP) complex of the simplest diphosphonate ligand. The bonding situations and natural bond orbital compositions were studied by the Mulliken population analysis (MPA) and natural bond orbital (NBO) analysis. The results indicate that the σ and π contributions to the Tc-O bonds are strongly polarized towards the oxygen atoms and the ionic contribution to the Tc-O bonding is larger than the covalent contribution. The electronic transitions investigated by TDDFT calculations and molecular orbital analyses show that the origin of all absorption bands is ascribed to the ligand-to-metal charge transfer (LMCT) character. The solvent effect on the electronic structures and absorption spectra has also been studied by performing DFT and TDDFT calculations at the B3LYP/6-31G*(cc-pVDZ-pp for Tc) level with the integral equation formalism polarized continuum model (IEFPCM) in different media. It is found that the absorption spectra display blue shift in different extents with the increase of solvent polarity.

Key Words : Technetium-diphosphonate complex, Density functional theory (DFT), Time-dependent density functional theory (TDDFT), Electronic structure, Absorption spectrum

Introduction

In the past few years, technetium (Tc) complexes have received considerable attention for their interesting physical, chemical, radiochemical and biological properties as well as their medical applications.[1-9] Particular interests have been devoted to the complexes containing the γ-emitting isotope ^{99m}Tc since they found very promising applications as diagnostic radiopharmaceuticals due to the favorable nuclear properties (E_γ = 142 keV, $t_{1/2}$ = 6.02 h), wide availability and low cost of the radionuclide ^{99m}Tc.[4-9] A variety of ^{99m}Tc-based radiopharmaceuticals have been developed and approved by the Federal Drug Administration (FDA) for determining organ function or assessing disease status by imaging methods.[7-9] Bone imaging agents are among the first developed ^{99m}Tc-based radiopharmaceuticals and among the most widely used radiopharmaceuticals in the diagnostic nuclear medicine,[7] which involve the coordination of ^{99m}Tc to diphosphonates such as methylenediphosphonate (MDP)[10] and hydroxymethylenediphosphonate (HMDP).[11] They have been used for many years in bone scanning and provided an effective means of diagnosing primary bone cancer, metastatic bone disease, Paget's disease, osteoporosis and bone trauma.

Recently, a series of novel ^{99m}Tc-diphosphonate complexes have been extensively reported experimentally.[12] We have also been involved for several years in the synthesis and biological evaluation of novel ^{99m}Tc-diphosphonate complexes for developing novel potential bone imaging agents.[13] Despite the importance and widespread clinical use of these complexes, however, almost no definitive information is available as to their structures. Even for the complex ^{99m}Tc-MDP (Scheme 1), where MDP is the simplest member of the diphosphonate ligands used in the preparation of ^{99m}Tc-based bone imaging agents, very little is actually known about its formulation and structure. This is largely because that ^{99m}Tc is available at tracer levels, which does not permit characterization of the complex by routine spectroscopic and analytical methods. This lack of fundamental chemical information not only restricts the development of improved ^{99m}Tc-diphosphonates, but also severely hinders the development of analogous diphosphonate formulations containing β-emitting radionuclides such as ^{186}Re, which could be used for the treatment of metastatic bone cancer.[4,8]

In fact, over the past several years considerable effort has been devoted to understanding the fundamental chemistry of ^{99m}Tc/^{186}Re-diphosphonate radiopharmaceuticals.[14] For ex-

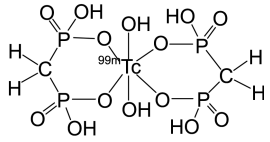

Scheme 1

ample, Libson *et al.*[14a] have prepared and characterized the structure of the stable ^{99}Tc-MDP complex for investigating the structure of the bone imaging agent ^{99m}Tc-MDP. Martin and co-workers[14b] have studied the structures of ^{99}Tc-MDP in aqueous solution by an EXAFS (extended X-ray absorption fine structure) analysis. Elder *et al.*[14c] also studied the structure and composition of Re-HEDP as an analogue of the radiotherapeutic agent ^{186}Re-HEDP by EXAFS spectroscopy. Recently, molecular modeling and quantum chemical (QM) calculation have been carried out by us to predict the structure and understand the fundamental chemistry of the metal-based diagnostic agent ^{99m}Tc-MDP.[14d] To the best of our knowledge, however, there are few studies on the metal-ligand bonding nature, electronic structure and spectral property of the ^{99m}Tc-diphosphonates in spite of the well-developed technetium chemistry with other ligands.

As well known, with the rapid development on the computer technology and theoretical chemistry, studies on the compounds could be facilitated and more economical with the computer modeling and simulating. These not only provide useful information that is difficult or impossible to measure, but also lead to a reduction in unnecessary measurement or synthesis of candidates in the course of designing new materials. Thus, it is necessary to perform a theoretical investigation on the title compound for further understanding its other physical, chemical, and radiochemical properties.

In this study, a detailed theoretical investigation on the electronic structures and absorption spectral property of the prototypical technetium-diphosphonate complex ^{99m}Tc-MDP was carried out using density functional theory (DFT)[15] and time-dependent density functional theory (TDDFT)[16] as an extension of previous studies on the complex ^{99m}Tc-MDP. Also, some comparisons have been made among different methods and different solvents. We hope the comparisons can indicate the effect of the basis set and the solvent on the electronic structures and absorption spectra, which will provide instructive information for the ongoing research on the ^{99m}Tc-based radiopharmaceuticals and could guide the molecular design and analysis of novel ^{99m}Tc-diphosphonate bone imaging agents.

Computational Methods

According to the previous studies on the complex ^{99m}Tc-MDP,[14d] two energetically most preferred isomers were selected for studying the electronic structure, absorption spectrum, and solvent effect as well as the basis set effect. They were fully optimized without any symmetry restrictions by the Berny method at the DFT-B3LYP level[17] with the LANL2DZ basis set.[18] To characterize the nature of the stationary point, harmonic vibrational analysis was performed subsequently on each optimized structure at the same level. For comparison and investigation of the basis set effect, the basis sets 6-31G*(LANL2DZ for Tc),[19] 6-31G* (cc-pVDZ-pp for Tc)[20] and DGDZVP[21] were also used in combination with the B3LYP functional to study the structure and properties of ^{99m}Tc-MDP. The bonding interactions and natural bond orbital compositions were studied and analyzed by the Mulliken population analysis (MPA)[22] and natural bond orbital (NBO) analysis.[23] The electron density diagrams of molecular orbitals were generated with the GaussView graphics program.[24]

On the basis of the optimized ground-state geometries, TDDFT[16] calculations were performed at the same level of accuracy as specified above to investigate the absorption properties of the title complex. In addition, the solvent effect on the electronic structures and spectral properties of the title complex was also studied by performing self-consistent reaction field (SCRF) calculations using the integral equation formalism polarized continuum model (IEFPCM).[25] The solute-solvent boundary was defined by using a solvent excluding surface, and the solute surface was defined by using the United Atom Topological model for the radii of the solute atoms. Six solvent models were employed: cyclohexane (ε = 2.023, R_{solv} = 2.815 Å), dichloroethane (ε = 10.36, R_{solv} = 2.505 Å), ethanol (ε = 24.55, R_{solv} = 2.18 Å), acetonitrile (ε = 36.64, R_{solv} = 2.155 Å), dimethylsulfoxide (ε = 46.7, R_{solv} = 2.455 Å), and water (ε = 78.39, R_{solv} = 1.385 Å), where ε is the dielectric constant and R_{solv} is the sphere radius of the solvent.

All calculations were performed with the Gaussian03 program package[26] on a DELL PE 2850 server and a Pentium IV computer, using the default convergence criteria given in the program.

Results and Discussion

Bonding Nature. The optimized structures of *cis* and *trans* isomers of the complex ^{99m}Tc-MDP are presented in Figure 1, showing one Tc center bridging two MDP ligands. The atomic numbering used in the text is also shown. The vibrational frequencies calculated on the basis of the optimized structures ascertain that they are stable (no imaginary frequencies) on their potential energy surfaces. To gain insight into the bonding situation existing in the title complex, theoretical studies on the electronic properties of the equilibrium geometry by means of Mulliken population analysis. As known, the MPA overlap populations reflect the electron accumulations between two atoms which are usually regarded to be a measure of the bond character and strength. In general, positive and negative values of overlap population correspond to the bonding and antibonding states, respectively. A value close to zero indicates that there is no significant interaction between two atoms.

In Table 1, the MPA overlap populations relative to the metal-ligand and phosphorus-ligand bondings are listed. As for the *cis* isomer of the title complex, the overlap populations between Tc and O of the MDP ligands (i.e., $P_{Tc\text{-}O2}$, $P_{Tc\text{-}O6}$, $P_{Tc\text{-}O7}$, $P_{Tc\text{-}O11}$) are found to be 0.112-0.228 while those in the *trans* isomer are 0.126-0.231, which both decrease in the order of 6-31G*(cc-pVDZ-pp for Tc) > LANL2DZ > 6-31G*(LANL2DZ for Tc) > DGDZVP. At the same calculation level, the corresponding values of the

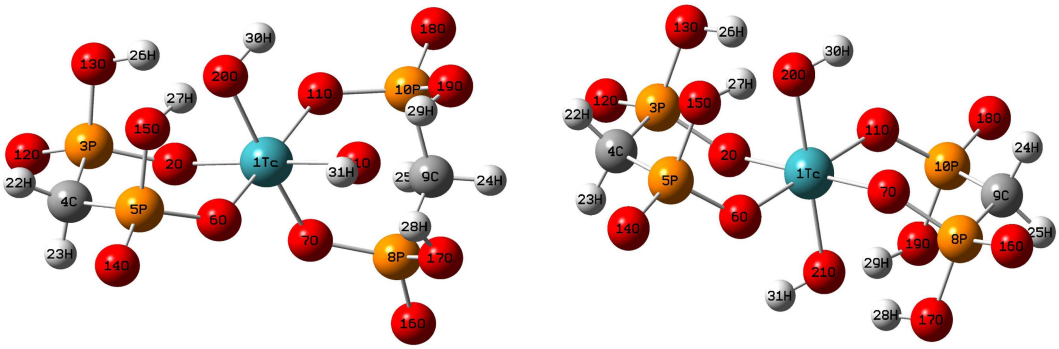

Figure 1. Optimized structures of the stable *cis*- (left) and *trans*-^{99m}Tc-MDP (right) at the B3LYP/LANL2DZ level.

Table 1. Bonding overlap population ($P_{X\text{-}Y}$) and Wiberg bond index ($W_{X\text{-}Y}$) of *cis*- and *trans*-^{99m}Tc-MDP obtained from MPA and NBO analyses at different DFT levels[a]

MPA	*cis*-^{99m}Tc-MDP				*trans*-^{99m}Tc-MDP			
	A	B	C	D	A	B	C	D
$P_{Tc\text{-}O2}$	0.162	0.151	0.228	0.118	0.177	0.152	0.231	0.126
$P_{Tc\text{-}O6}$	0.173	0.144	0.228	0.123	0.177	0.152	0.231	0.126
$P_{Tc\text{-}O7}$	0.162	0.143	0.216	0.112	0.177	0.152	0.231	0.126
$P_{Tc\text{-}O11}$	0.173	0.158	0.228	0.126	0.177	0.152	0.231	0.126
$P_{Tc\text{-}O20}$	0.145	0.114	0.169	0.157	0.130	0.113	0.165	0.113
$P_{Tc\text{-}O21}$	0.145	0.141	0.215	0.162	0.130	0.113	0.165	0.113
$P_{P3\text{-}O2}$	0.039	0.292	0.266	0.340	0.033	0.283	0.253	0.319
$P_{P3\text{-}O12}$	0.480	0.636	0.649	0.673	0.479	0.633	0.647	0.670
$P_{P3\text{-}O13}$	0.092	0.281	0.267	0.318	0.094	0.286	0.268	0.311
$P_{C4\text{-}P3}$	-0.109	0.213	0.199	0.271	-0.104	0.217	0.201	0.293
NBO	*cis*-^{99m}Tc-MDP				*trans*-^{99m}Tc-MDP			
	A	B	C	D	A	B	C	D
$W_{Tc\text{-}O2}$	0.604	0.535	0.518	0.439	0.554	0.548	0.535	0.488
$W_{Tc\text{-}O6}$	0.550	0.556	0.539	0.394	0.554	0.548	0.535	0.488
$W_{Tc\text{-}O7}$	0.604	0.479	0.469	0.374	0.554	0.548	0.535	0.488
$W_{Tc\text{-}O11}$	0.550	0.514	0.509	0.499	0.554	0.548	0.535	0.488
$W_{Tc\text{-}O20}$	0.461	0.551	0.553	0.643	0.493	0.526	0.529	0.494
$W_{Tc\text{-}O21}$	0.461	0.610	0.609	0.591	0.493	0.526	0.529	0.494
$W_{P3\text{-}O2}$	0.758	0.814	0.817	0.849	0.754	0.793	0.797	0.809
$W_{P3\text{-}O12}$	1.217	1.244	1.233	1.183	1.212	1.244	1.239	1.198
$W_{P3\text{-}O13}$	0.702	0.712	0.710	0.725	0.708	0.721	0.719	0.717
$W_{C4\text{-}P3}$	0.799	0.763	0.766	0.784	0.800	0.768	0.769	0.812

[a]A, B, C, and D denote the calculations at the B3LYP/LANL2DZ, B3LYP/6-31G*(LANL2DZ for Tc), B3LYP/6-31G*(cc-pVDZ-pp for Tc), and B3LYP/DGDZVP levels, respectively.

cis isomer are smaller than those of the *trans*, indicating the bonding interactions between these atoms in the former are weaker than those in the latter. On the contrary, the overlap populations between Tc and O of the hydroxy ligands (i.e., $P_{Tc\text{-}O20}$, $P_{Tc\text{-}O21}$) in the *cis* isomer (0.114-0.215) are larger than those in the *trans* isomer (0.113-0.165), suggesting that these bonding interactions in the former are stronger than those in the latter.

On the other hand, the chemical bonding in transition metal complexes is usually described in terms of ionic and covalent interactions between the metal and the ligands. In many transition metal complexes (especially complexes of first-row transition metals), the ionic contribution to metal-ligand bonding is thought to be dominant. However, in the title complex the metal-oxygen bonding also has a significant covalent contribution in addition to the ionic contribution. This is reflected in the metal-oxygen orbital mixing (see Figure 4 and Figures S1-S3 of the Supporting Information). And a high bond overlap population indicates a high degree of covalency in the bond (see Table 1). The ionic contribution is related to the atomic charges of the metal (*ca.* 1.3 e) and the oxygen atoms of the ligand (*ca.* –0.7 e). Furthermore, from the MPA and NPA (natural population analysis)[27] derived partial charges of selected atoms in the free ligand OH and MDP as well as the complex Tc-MDP (Table 2) one can find that the partial negative

Table 2. MPA- and NPA-derived Atomic charges at the B3LYP/LANL2DZ level[a]

Atom	MPA				NPA			
	OH	MDP	*cis*-Tc-MDP	*trans*-Tc-MDP	OH	MDP	*cis*-Tc-MDP	*trans*-Tc-MDP
Tc(1)			1.292	1.278			1.634	1.639
O(2)		−0.799	−0.746	−0.752		−1.049	−1.024	−1.029
O(6)		−0.785	−0.758	−0.752		−1.047	−1.036	−1.029
O(7)			−0.758	−0.752			−1.024	−1.029
O(11)			−0.746	−0.752			−1.036	−1.029
O(12)		−0.646	−0.726	−0.730		−1.002	−1.066	−1.070
O(13)		−0.699	−0.744	−0.750		−1.027	−1.058	−1.061
O(14)		−0.653	−0.728	−0.730		−1.006	−1.069	−1.070
O(15)		−0.674	−0.755	−0.750		−1.026	−1.066	−1.061
O(16)			−0.726	−0.730			−1.066	−1.070
O(17)			−0.744	−0.750			−1.058	−1.061
O(18)			−0.728	−0.730			−1.069	−1.070
O(19)			−0.755	−0.750			−1.066	−1.061
O(20)	−1.133		−0.817	−0.821	−1.311		−1.047	−1.027
O(21)			−0.817	−0.821			−1.047	−1.027
P(3)		1.315	1.348	1.348		2.262	2.290	2.291
P(5)		1.299	1.337	1.348		2.246	2.288	2.291
P(8)			1.337	1.348			2.29	2.291
P(10)			1.348	1.348			2.288	2.291
C(4)		−0.843	−0.890	−0.895		−1.164	−1.175	−1.176
C(9)			−0.890	−0.895			−1.175	−1.176

[a]A, B, C, and D denote the calculations at the B3LYP/LANL2DZ, B3LYP/6-31G*(LANL2DZ for Tc), B3LYP/6-31G*(cc-pVDZ-pp for Tc), and B3LYP/DGDZVP levels, respectively.

charges on the hydroxy oxygens (O20, O21) range from −1.13/−1.31 to −0.82/−1.04 e as the free OH coordinates the Tc(IV) center to yield the *cis*- and *trans*-Tc-MDP. The increase in the oxygen charges certainly leads to the reduction in the formal charge of Tc(IV). Besides, the partial charges on the carbon, oxygen and phosphorus in the free MDP all change greatly in the coordinated complex, which also result in the change of the formal charge of Tc(IV). All these can likely be attributed to the nephelauxetic effect, whereby the ligand electron donation partially shields the metal d electrons from the central-ion nuclear charge and drives expansion of the d-electron "cloud".[28] This also agrees well the conclusion drawn by Pauling[29] that "Stable M-L bond formation generally reduces the positive charge on the metal as well as the negative charge on the ligand."

Inspecting the overlap populations of P-O and P-C bonds, we can draw a conclusion that the bonding interactions between P3 and O2, O12 in the *cis* isomer are slightly larger than those in the *trans* one while those between P3 and O13, C4 in the former are slightly smaller than those in the latter. Noteworthy is that the bonding overlap populations of P3-O12 are over two times larger than those of P3-O2, P3-O13 and P3-C4 except those obtained at the B3LYP/LANL2DZ level are abnormal, indicating P3-O12 possesses double bond character. This is in line with the geometric parameter analysis of the P-O bond in previous experimental and theoretical studies.[14a,30]

Although MPA can provide a correct global trend, it suffers from some shortcomings especially the basis set dependence and NBO is much more reliable.[31] Therefore, in order to gain reliable bonding features, the extent of bonding interaction between atom centers in *cis*- and *trans*-^{99m}Tc-MDP was further investigated using NBO theory. The conventional parameters have been analyzed such as bond order and NBO distribution, which are frequently used to characterize the bonding situation in the molecule.

The calculated Wiberg bond indices (WBI)[32] are listed in Table 1. The results indicate that six Tc-O bonds and P3-O2, P3-O13, P3-C4 all possess single-bond character while P3-O12 exhibits double-bond character, consistent with the conclusions drawn from the MPA overlap populations and geometrical parameters. And the higher bond order of P-O bonds suggests that they are stronger than the Tc-O bonds. Similarly, from the WBI values we can conclude that the bond strengths of Tc-O2, Tc-O6, Tc-O7, Tc-O11, P3-O13 and P3-C4 in the *cis* isomer are stronger than those of the *trans* isomer, while those of Tc-O20, Tc-O21, P3-O2 and P3-O12 are weaker in the former than in the latter. With the basis set ranging, the bond orders between Tc and O of the MDP ligands are found to decrease in the order of LANL2DZ > 6-31G*(LANL2DZ for Tc) > 6-31G*(cc-pVDZ-pp for Tc) > DGDZVP for both isomers, while other bond orders vary diversely. The WBI of the *trans* isomer is also symmetrical as the Mulliken populations due to its C_{2h} symmetry. These electronic features can be observed intuitively from Figure 2, which compares the bonding interactions in the *cis*- and *trans*-^{99m}Tc-MDP at different levels of DFT theory from the MPA and NBO analyses.

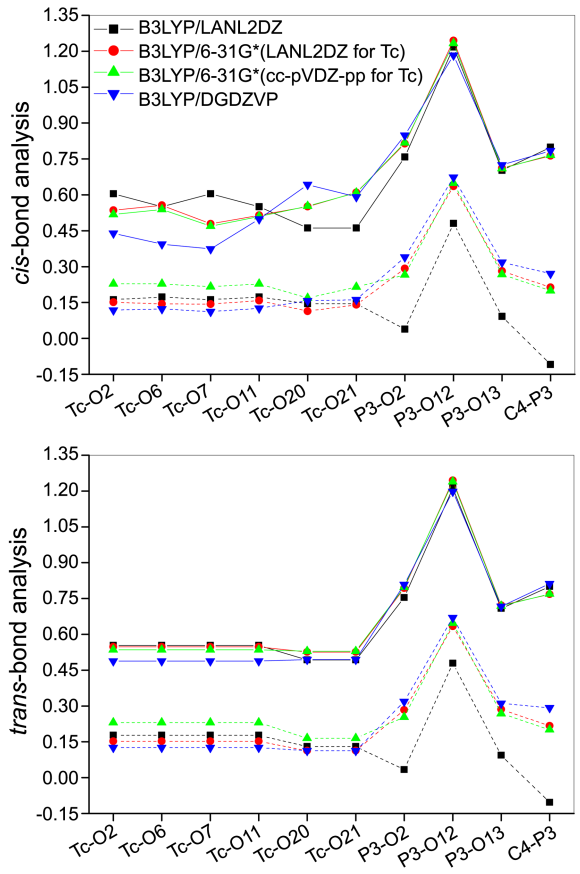

Figure 2. Bond overlap populations (dash line) and bond orders (solid line) of the *cis*- and *trans*-^{99m}Tc-MDP at different levels of DFT theory.

In Table 3 the bond nature analysis for the core $[TcO_6]^{2-}$ as obtained using B3LYP/6-31G*(cc-pVDZ-pp for Tc) is shown (the results obtained with other methods are included in the Supporting Information, Tables S1-S3). Inspection of natural hybrid orbital (NHO) compositions and occupancies suggests that the bonding interactions between the Tc and O centers are σ and π symmetry for both isomers. In all the NHO, the polarization coefficients between the Tc and O centers are significantly different, which suggest that the ionic contribution plays a dominant role in determining the overall strength of the metal-ligand bonding interaction. In the case of *cis*-^{99m}Tc-MDP, the Tc-O σ bonds are strongly polarized towards the oxygen atoms; the metal contributions to these bonds are between 12.98% and 18.02%. The Tc-O π bonds are even more polarized and the metal contributions are only between 6.51% and 8.22%. The *s* and particularly the *p* contributions characterize the Tc-O bond as a donor-acceptor bond. The hybridization at technetium shows clearly that the *d*-orbital contribution dominates the Tc-O σ and π bonds. With respect to the *trans*-^{99m}Tc-MDP, the same is true. The hybridization at the metal atom shows mainly *d* character and at the non-metal exhibits mainly *p* character. A strong polarization toward the non-metal was detected in the Tc-O σ bonds, the contributions of technetium ranging from 10.47% to 16.48%. And more polarization toward the non-metal was also detected in the Tc-O π bond with the metal contribution of only 8%. This description of the Tc-O bonds is in agreement with the results of a few studies regarding the analysis of the bonding situation in transition metal oxido complexes.[33]

Absorption Spectrum. In principle, the study of spectroscopic and photophysical properties as a function of ligand substituents can give insight into nature of the ground and excited states.[34,35] It is known that DFT has become a useful tool in evaluating ground-state properties with an accuracy close to that of post-HF methods, and there is increasing interest in extending DFT to excited electronic states.[35] Essentially they clarified the distinct nature of the transitions that yield the peculiar characteristics of the compounds. Nevertheless, very little experimental and theoretical work is yet available on this topic of ^{99m}Tc-MDP despite the potential interest of an advanced quantum chemical approach for a better understanding of key issues, like the nature of both the ground and the excited states involved in the absorption and emission. Therefore, it is of great significance to study the spectral properties of ^{99m}Tc-MDP.

The calculated excitation energies (E) associated with their oscillator strengths (f), wavelengths (λ), and the main configurations of the *cis*-^{99m}Tc-MDP and *trans*-^{99m}Tc-MDP at the B3LYP/6-31G*(cc-pVDZ-pp for Tc) level are given in Table 4 as well as their assignments. The results obtained at other levels are presented in Tables S4-S6 of the Supporting Information. For clarity, only transitions with the oscillator strength larger than 0.0020 are included. For all transitions, only orbital contributions larger than 10% are taken into account. Figure 3 shows the absorption spectra of two isomers at different DFT levels, which are simulated by taking all transitions into account with a global half-band width of 10 cm^{-1}. Since there are no corresponding experimental values, we cannot make any comparison. We hope that our results will be used as reference data and helpful for the future investigation of technetium-diphosphonate complexes.

At first, by comparing the absorptions of *cis*-^{99m}Tc-MDP and *trans*-^{99m}Tc-MDP, it is indicated that the variation of the coordination site of the substituent changes the excitation energy and spectral property to a different extent. As shown in Figure 3, the *cis* isomer has one intense electron transition band along with an absorption band as a shoulder and the *trans* isomer has two intense electron transition bands. At the same calculational level, locations of the peaks are extremely near for the *cis* and *trans* isomers, but the intensities of two peaks of the *trans* isomer are lower than the corresponding peaks of the *cis* isomer.

Inspecting Table 4, it can be found that in the case of the *cis* isomer, the lowest energy absorption band located at 311 nm (f = 0.0038) as obtained from the B3LYP/6-31G* (LANL2DZ for Tc) methodology, which can be described by the transitions βHOMO-4 → βLUMO, βHOMO-7 → βLUMO, and βHOMO-3 → βLUMO. Analysis of these frontier molecular orbitals (MOs) shows that the electron density is transferred from the phosphorus and oxygen donor atoms in the MDP ligand to the center metal Tc (see Figure

Table 3. NHO composition of selected NBOs of *cis*- and *trans*-^{99m}Tc-MDP at the B3LYP/6-31G*(cc-pVDZ-pp for Tc) level[a]

Bond	Occupancy	%Tc	%O	%ns	%np	%(n-1)d	%(n-2)f
			cis-^{99m}Tc-MDP				
Tc-O2	0.95 (beta)	7.36 (0.271)		0.55	1.14	97.94	0.37
			92.64 (0.962)	0.02	99.92	0.07	
Tc-O6	0.97 (alpha)	15.67 (0.396)		33.43	0.45	65.90	0.22
			84.33 (0.918)	23.97	75.99	0.04	
Tc-O7	0.96 (beta)	8.22(0.287)		0.84	1.77	96.98	0.40
			91.78(0.958)	1.06	98.89	0.05	
Tc-O11	0.97 (beta)	12.98 (0.360)		33.86	0.50	65.40	0.24
			87.02 (0.933)	20.10	79.85	0.04	
	0.95 (beta)	6.51 (0.255)		0.03	1.55	97.98	0.44
			93.49 (0.967)	0.00	99.94	0.06	
Tc-O20	0.99 (alpha)	16.88 (0.411)		32.64	0.53	66.64	0.19
			83.12 (0.912)	20.91	79.04	0.05	
	0.99 (beta)	14.36 (0.379)		32.84	0.48	66.46	0.22
			85.64 (0.925)	23.81	76.14	0.05	
Tc-O21	0.99 (alpha)	18.02 (0.424)		32.15	0.53	67.12	0.21
			81.98 (0.905)	20.17	79.77	0.06	
	0.99 (beta)	15.35 (0.392)		30.41	0.57	68.80	0.23
			84.65 (0.920)	25.08	74.86	0.06	
			trans-^{99m}Tc-MDP				
Tc-O2	0.97 (beta)	14.19 (0.377)		24.72	0.26	75.02	
			85.81 (0.926)	18.55	81.41	0.04	
	0.95 (beta)	8.00 (0.283)		0.49	0.71	98.81	
			92.00 (0.959)	0.01	99.93	0.06	
Tc-O6	0.96 (beta)	14.41 (0.379)		24.72	0.27	75.02	
			85.59 (0.925)	17.54	82.31	0.12	
Tc-O7	0.97 (alpha)	15.84 (0.398)		32.47	0.27	67.26	
			84.16 (0.917)	23.41	76.56	0.03	
Tc-O11	0.97 (alpha)	15.84 (0.398)		32.47	0.27	67.26	
			84.16 (0.917)	23.40	76.57	0.03	
Tc-O20	0.98 (alpha)	16.48 (0.406)		33.19	0.56	66.25	
			83.52 (0.914)	19.83	80.13	0.04	
	0.99 (beta)	14.18 (0.377)		28.62	0.43	70.95	
			85.82 (0.926)	24.88	75.08	0.04	
Tc-O21	0.80 (beta)	10.47 (0.323)		0.49	0.71	98.81	
			89.53 (0.946)	14.38	84.84	0.78	

[a]%Tc and %O give the contributions of the bond at technetium and oxygen, respectively. %ns, %np, %(n-1)d and %(n-2)f give the hybridization of the bond. Data in the parentheses are the polarization coefficients of Tc and O. For each bond, in the first and second rows the hybridization at the metal and non-metal respectively are given.

4). This indicates that the transition bears a significant ligand-to-metal charge transfer (LMCT) character. In the same spectrum, the intense absorption band at 282 nm (f = 0.0131) is mainly originated from two transitions βHOMO-3 → βLUMO+1 and βHOMO-1 → βLUMO+2, which can also be assigned to the LMCT character (see Figure 4). This also reflects from another side that the analysis of MOs is not only relevant to gain insight into the chemical bonding between the metal atom and the ligands, but also instructive for the further understanding of the optical properties.

In the case of the *trans* isomer, the calculated transition gives rise to the lowest energy absorption band and intense absorption band at 322 nm (f = 0.0036) and 290 nm (f = 0.0124), respectively, which are mainly attributed to the transitions βHOMO-2 → βLUMO and βHOMO-2 → βLUMO+2. They are principally ascribed to the redistribution of the electron density between the MDP-based MOs and the metal Tc-centered MOs. In other words, they are also assigned to the LMCT character. In summary, although the different coordination site of the hydroxyl group in the *cis* and *trans* isomers of the title complex leads to different transition intensities with different transition MOs, it does not significantly change the electron transition model.

Taking the basis set effect into account, in both absorption spectra of *cis* and *trans* isomers important red-shifts are detected on going from the basis set 6-31G*(cc-PVDZ-pp

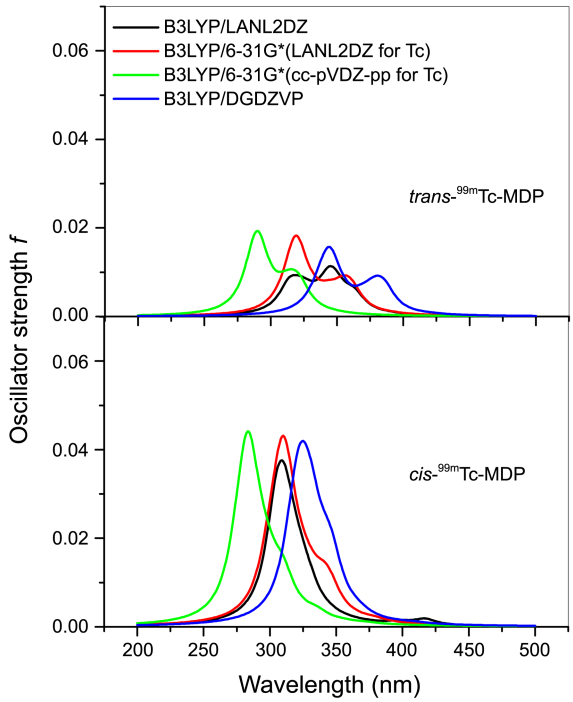

Figure 3. Absorption spectra of *cis*- and *trans*-^{99m}Tc-MDP calculated at different levels of DFT theory.

for Tc) to 6-31G*(LANL2DZ for Tc) to LANL2DZ and to DGDZVP (see Figure 3). Meanwhile, the intensities of the absorption bands decrease in the order of 6-31G*(cc-PVDZ-pp for Tc) > 6-31G*(LANL2DZ for Tc) > DGDZVP > LANL2DZ. The molecular orbitals active in the electronic transitions of *cis*- and *trans*-^{99m}Tc-MDP at the B3LYP/LANL2DZ, B3LYP/6-31G*(LANL2DZ for Tc), and B3LYP/DGDZVP levels are displayed in Figures S1-S3 of the Supporting Information, respectively. One can see that at different levels the HOMOs in both isomers are nearly completely localized on the MDP moiety and the hydroxyl, while the LUMOs are almost predominately localized on the center metal Tc. This indicates that electronic transitions corresponding to the absorption spectra of the title complex at other DFT levels are also mainly assigned to the LMCT character.

Solvent Effect.

Solvent Effect on Energy: As known, the order and composition of frontier molecular orbitals (FMOs) of the anion is an important factor in determining their reactivity, redox properties, and excited-state structures. However, it is also acknowledged that the highly charged anion does not exist in the gas phase; moreover, FMOs of the negatively charged system are sensitive to the size of the basis set.[36] Thus, based on the gas-phase optimized ground-state structures, single point energy calculations were carried out for the *cis* and *trans* isomers of the complex ^{99m}Tc-MDP with the IEFPCM model. Six solvent models and a larger size basis set 6-31G*(cc-pVDZ-pp for Tc) were employed for solvent and basis considerations.

Table 5 gives the total electronic energies and FMO energies of the *cis*- and *trans*-^{99m}Tc-MDP in cyclohexane, dichloroethane, ethanol, acetonitrile, dimethylsulfoxide, and water solvents as well as in the gas-phase. The stabilization

Table 4. Dominant optical transition characters for the lowest excitation states of the *cis*- and *trans*-^{99m}Tc-MDP, employing the B3LYP/6-31G*(cc-pVDZ-pp for Tc) method[a]

E/eV	λ/nm	f	Transition orbital	Assignment
			cis-^{99m}Tc-MDP	
4.51	275.12	0.0049	98 → 107B, 101 → 107B, 103 → 107B	H-6 → L+2B, H-3 → L+2B, H-1 → L+2B
4.43	279.74	0.0037	100 → 107B, 103 → 107B, 97 → 107B	H-4 → L+2B, H-1 → L+2B, H-7 → L+2B
4.39	282.13	0.0131	101 → 106B, 103 → 107B	H-3 → L+1B, H-1 → L+2B
4.38	283.12	0.0023	102 → 107B, 103 → 107B	H-2 → L+2B, H-1 → L+2B
4.37	283.51	0.0028	97 → 105B, 98 → 106B, 100 → 105B	H-7 → LB, H-6 → L+1B, H-4 → LB
4.36	284.62	0.0112	101 → 107B, 101 → 106B, 103 → 107B, 100 → 107B	H-3 → L+2B, H-3 → L+1B, H-1 → L+2B, H-4 → L+2B
4.33	286.53	0.0039	98 → 106B, 102 → 107B	H-6 → L+1B, H-2 → L+2B
4.27	290.06	0.0023	103 → 106B, 100 → 106B	H-1 → L+1B, H-4 → L+1B
4.19	296.08	0.0021	105 → 109A, 102 → 106B	H-2 → L+1A, H-2 → L+1B
4.01	309.05	0.0021	102 → 105B, 104 → 107B	H-2 → LB, H → L+2B
3.99	310.80	0.0038	100 → 105B, 97 → 105B, 101 → 105B	H-4 → LB, H-7 → LB, H-3 → LB
			trans-^{99m}Tc-MDP	
4.33	286.10	0.0026	101 → 106B	H-3 → L+1B
4.28	289.91	0.0124	102 → 107B	H-2 → L+2B
4.26	291.01	0.0021	102 → 106B, 101 → 107B	H-2 → L+1B, H-3 → L+2B
3.99	310.72	0.0021	104 → 106B	H → L+1B
3.91	317.42	0.0035	101 → 105B	H-3 → LB
3.85	322.27	0.0036	102 → 105B	H-2 → LB

[a]H = HOMO, L = LUMO, H-1 = HOMO-1, L+1 = LUMO+1, etc; A and B denote the α- and β-spin molecular orbitals, respectively.

energy by solvent was calculated as the relative energies of the *cis* and *trans* conformations in the solvent to those in the gas phase, i.e., $\Delta E_{sol} = E_T^{sol} - E_T^{gas}$; and therefore a negative ΔE_{sol} indicates that the conformation in the solvent is more stable than that in the gas-phase.

According to our calculations, it was found that the solvent effect significantly decreased the total energies E_T and the solvent stabilization energy ΔE_{sol} of the *cis* and *trans* isomers, suggesting both of them in the solvent are more stable than in the gas phase. Especially as the medium ranges from the gas-phase to cyclohexane to dichloroethane, the decreasing amplitude for the E_T and ΔE_{sol} was remarkably large for both isomers. However, as the solvent changing from the dichloroethane to water with the polarity

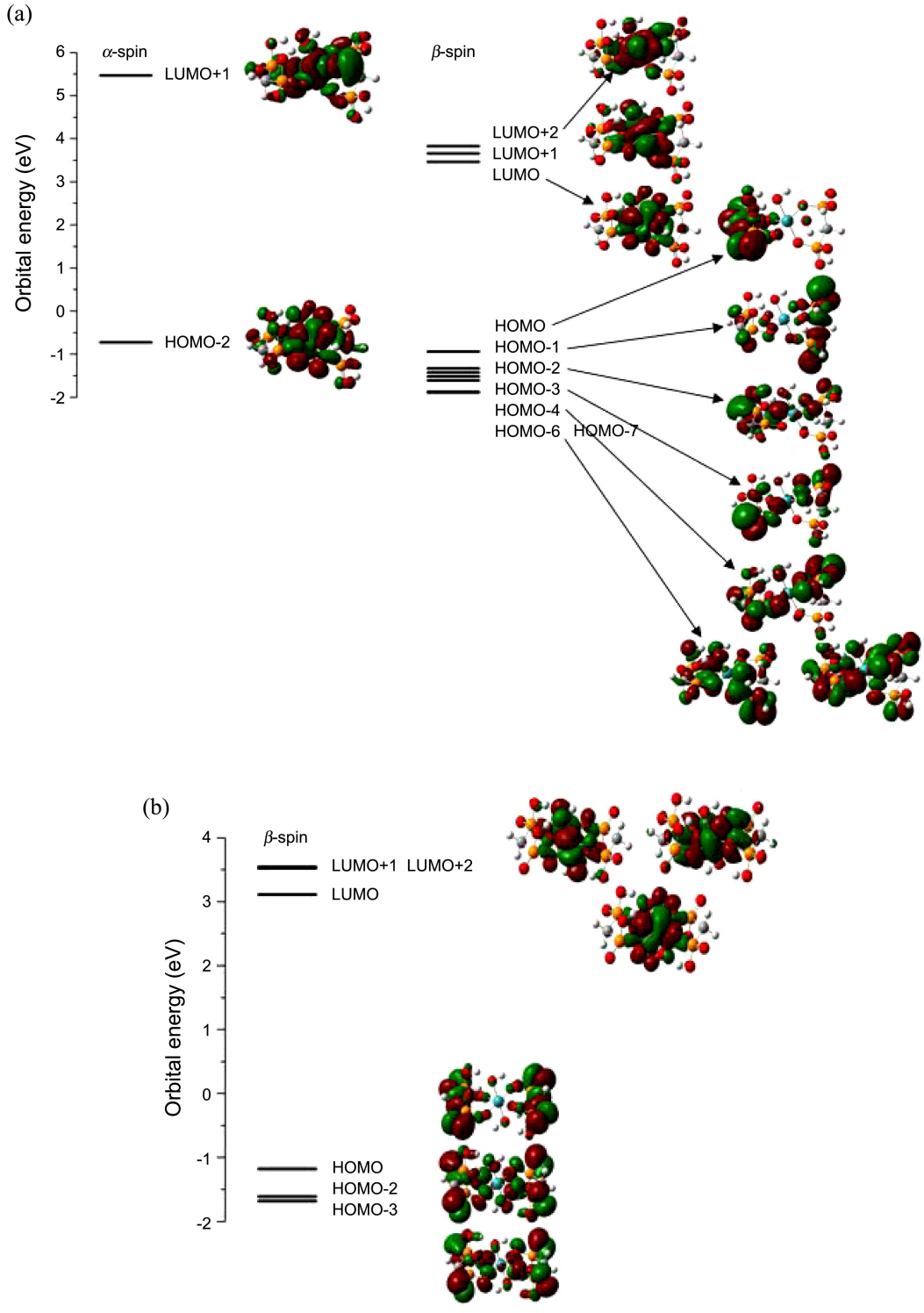

Figure 4. Molecular orbitals active in the electronic transitions of *cis*-^{99m}Tc-MDP (a) and *trans*-^{99m}Tc-MDP (b) obtained at the B3LYP/6-31G*(cc-pVDZ-pp for Tc) level.

increasing, E_T and ΔE_{sol} decreased slightly. These results suggest that *cis* and *trans* isomers of ^{99m}Tc-MDP are easy to dissolve in polar solvents and more stable in more polar solvent, but the solvent effect is more obvious with the smaller polarity. The FMO energies of *cis* and *trans* isomers also give the same feature. But the energy gap ΔE_g between these FMOs almost did not change when compared with those in the gas phase. For example, the HOMO-LUMO gaps of *cis* and *trans* isomers in the gas phase are 0.136 and 0.133 a. u. respectively, whereas those in the solvents are 0.138 and 0.136 a. u. respectively. In addition, we did not observe any distinct difference in the order and composition of FMOs between the gas phase and solvents. Therefore, it is concluded that studying the electronic structure of the gas-phase anion may be enough to understand the reactivity and excited-state structures of the title complex. The same conclusion has been obtained for other transition metal complexes.[36]

Here, it should be noted that the energy difference between the *cis* and *trans* isomers is relatively small and it decreases with the increasing solvent polarity. Therefore, a crucial question, how to prepare or separate the title compound with only one configuration in a practical way, still requires further studies.

Moreover, the solvent effect makes the dipole moment of the *cis* isomer increase with the solvent polarity increasing, indicating that the polarity of *cis*-^{99m}Tc-MDP increases with the increasing solvent polarity. This is attributed to the inductive effect of the solvent. As for the *trans* isomer, it keeps *ca*. 0 Debye in different solvents due to its C_{2h} symmetry, indicating its polarity is very small in different media. It was also found that the solvent effect on the stabilization energy is in parallel with that on the dipole moment of the *cis* isomer. And there is a good linear relationship between the solvent stabilization energies and the dipole moments of *cis* isomer in the set of solvents with the correlation coefficient of –0.99. That is, the stronger the solvent polarity is, the larger the dipole moment of solute is, and the higher the stabilization energy is.

Solvent Effect on Absorption Spectrum: Although the above study indicates the study of the electronic structure of the gas-phase anion may be enough to understand the excited-state structures of the title complex, it is generally acknowledged that different solvents can cause different excitation energy and absorption spectrum because of the solvent polarity. In general trends, the absorption spectra of mononuclear compounds are more affected with solvent polarity than binuclear complexes.[37] So, it is necessary to discuss the absorption change of the title complex caused by the solvent polarity.

Figure 5 illustrates the different solvent effect on the absorption spectra of *cis*- and *trans*-^{99m}Tc-MDP intuitively, where the absorptions were calculated with the IEFPCM method in cyclohexane, dichloroethane, ethanol, acetonitrile, dimethylsulfoxide, and water at the B3LYP/6-31G*(cc-pVDZ-pp for Tc) level. It is obviously that compared with the absorption spectra of both isomers in the gas phase, the solvent leads to a blue shift in the absorption band and increase in the intensity of electron transitions. As the solvent polarity increases, on the whole, a small blue shift is observed in the lowest energy absorption band and intense electron transition band, which agrees well with the experimental observation on other complexes.[37] However, as the solvent polarity increases to 4.30 (ethanol), no important shifts can be detected in the absorptions even further increasing the solvent polarity. In other words, ranging from ethanol to water the solvent has little effect on the absorption bands of the *cis*- and *trans*-Tc-MDP. This is consistent well with the changes of solvent stabilization energies ΔE_{sol}, which are negligible in the polar solvents (ethanol, acetonitrile, dimethylsulfoxide and water) although their dielectric constants are significantly different.

Here, the solvent effect can be explained by the multiparametric method of Kamlet and Taft[38] in which the absorption and emission energies are correlated with different solvent properties according to the following equation, which is one of the most widely applied:[37]

$$\bar{\nu} = \bar{\nu}_0 + a\alpha + b\beta + p(\pi^* + d\delta)$$

where $\bar{\nu}_0$ is the value of the absorption or emission energies

Table 5. Solvent effect on the electronic structures of *cis*- and *trans*-^{99m}Tc-MDP employing the B3LYP/6-31G*(cc-pVDZ-pp for Tc) method[a]

Media[b]	E_T/a.u.		ΔE_{sol}/kcal·mol^{-1}		E_H/a.u.		E_L/a.u.		ΔE_g/a.u.		μ/Debye	
	cis	*trans*	*cis*	*trans*	*cis*	*trans*	*cis*	*trans*	*cis*	*trans*	*cis*	*trans*
g	–2581.9048964	–2581.9179422			–0.009	–0.019	0.127	0.114	0.136	0.133	5.284	0.001
c	–2582.0327801	–2582.0430043	–80.25	–78.48	–0.120	–0.129	0.016	0.006	0.136	0.135	5.867	0.001
d	–2582.1437157	–2582.1506505	–149.86	–146.03	–0.210	–0.215	–0.072	–0.079	0.138	0.136	6.713	0.004
e	–2582.1614085	–2582.1676933	–160.96	–156.72	–0.223	–0.227	–0.085	–0.091	0.138	0.136	6.905	0.007
a	–2582.1659433	–2582.1717147	–163.81	–159.24	–0.226	–0.230	–0.088	–0.094	0.138	0.136	6.983	0.006
ds	–2582.1667253	–2582.1730147	–164.30	–160.06	–0.227	–0.231	–0.089	–0.095	0.138	0.136	6.972	0.006
w	–2582.1725509	–2582.1772313	–167.96	–162.71	–0.230	–0.234	–0.092	–0.098	0.138	0.136	7.068	0.011

[a] E_T, ΔE_{solv}, E_H, E_L, and ΔE_g denote the total energy, stabilization energy by solvent (the relative energy of the complex in a solvent to that in the gas phase), energy of the highest occupied molecular orbital (HOMO), energy of the lowest unoccupied molecular orbital (LUMO), and the energy gap between HOMO and LUMO ($\Delta E_g = E_L - E_H$), respectively. μ is the dipole moment. [b] g, c, d, e, a, ds, and w represent the results computed in the gas phase and different solvents with the increasing dielectric constant, i.e. cyclohexane (2.023), dichloroethane (10.36), ethanol (24.55), acetonitrile (36.64), dimethylsulfoxide (46.7), and water (78.39), respectively.

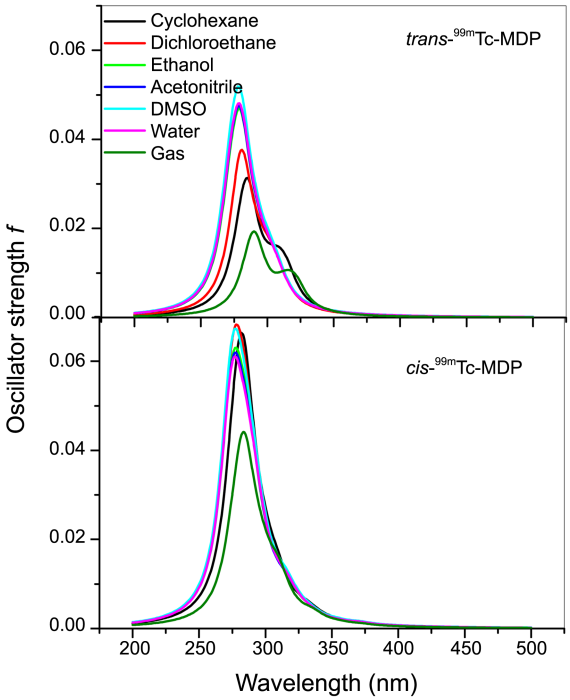

Figure 5. Normalized absorption spectra of *cis*- and *trans*-^{99m}Tc-MDP in different solvents and in the gas phase at the B3LYP/6-31G*(cc-pVDZ-pp for Tc) level.

in a reference solvent, α is an index of the solvent ability to act as a hydrogen-bond donor toward a solute, β is a measure of the ability of a bulk solvent to act as a hydrogen-bond acceptor, π^* is an index of the solvent polarity, and δ is the polarizability correction for different types of solvent that is usually negligible leading to a simplified equation. The parameters *a*, *b*, *p*, and *d* can be retrieved through a multi-parametric fitting on various solvents. With respect to the solvatochromism in the absorptions of *cis*- and *trans*-Tc-MDP, it is essentially reflected in the parameter β, i.e., higher sensitivity to the H-bond acceptor (or electron donor) strength of the solvent; and it is less sensitive to the polarity of the solvent (π^*). That is, the solvent effect on the absorption and energies is mainly due to the fact that intermolecular hydrogen-bonding interactions between the complex Tc-MDP and the solvent changes greatly from the nonpolar solvent (cyclohexane) to the polar solvent (dichloroethane, ethanol, acetonitrile, dimethylsulfoxide and water) whereas it changes slightly in different polar solvents.

Conclusions

The present work investigated the bonding situations and absorption spectra of *cis* and *trans* isomers of the typical technetium-diphosphonate complex ^{99m}Tc-MDP by DFT and TDDFT methods. The effect of basis set and solvent have also been studied. Major findings can be summarized as follows:

The bonding interactions between Tc and O of the MDP ligands in the *cis* isomer are weaker than those in the *trans*, while those between Tc and O of the hydroxy ligands in the former are stronger than those in the latter. The charge distribution reflects a significant ligand-to-metal electron donation, and NBO analysis indicates that the σ and π contributions to the Tc-O bonds are strongly polarized towards the oxygen atoms and the ionic contribution to the Tc-O bonding is larger than the covalent contribution. For both isomers, the origin of all absorption bands is ascribed to the LMCT character, where occupied oxygen-based orbitals and unoccupied technetium-centered orbitals are involved. Important red-shifts are detected for both isomers as the basis set ranging from 6-31G*(cc-PVDZ-pp for Tc) to 6-31G*(LANL2DZ for Tc) to LANL2DZ and to DGDZVP, and the intensities decrease in the order of 6-31G*(cc-PVDZ-pp for Tc) > 6-31G*(LANL2DZ for Tc) > DGDZVP > LANL2DZ.

Cis and *trans* isomers of ^{99m}Tc-MDP are easy to dissolve in polar solvents and more stable in a more polar solvent. The solvent effect also leads to a blue shift in the absorption spectrum of the title compound, where the shift becomes smaller and negligible with the increasing solvent polarity. These studies can provide deep insight into the electronic structures and absorption spectra of the complex ^{99m}Tc-MDP, which may be also instructive for the choice of solvent in future investigation of the spectral properties.

In addition, compared to all-electron basis sets, ECPs (effective core potentials) account to some extent for relativistic effects, which are believed to become important for the elements from the fourth row of the periodic table. Taking into account the computer resources and expended CPU time as well as the reliability of the calculated results, B3LYP/6-31G*(cc-PVDZ-pp for Tc) is suitable enough for studying the Tc-diphosphonate complexes in dealing with complicated electron correlation problems. This has a guiding role in the choice of method for further design and study of ^{99m}Tc-based radiopharmaceuticals.

Acknowledgments. We are very grateful for the financial support from the National Natural Science Foundation of China (20801024, 21001055), Natural Science Foundation of Jiangsu Province (BK2009077), and Science Foundation of Health Department of Jiangsu Province (H200963).

Supplementary Data. Plots of the active molecular orbitals in the electronic transitions of *cis*- and *trans*-^{99m}Tc-MDP calculated at other DFT levels (Figures S1-S3), the results of NBO analyses and TDDFT calculations for *cis*- and *trans*-^{99m}Tc-MDP at other DFT levels (Tables S1-S6).

References

1. Desmet, G., Myttenaere, C., Eds.; In *Technetium in the Environment*; Kluwer Academic Press: Dordrecht, 1986; p 420.
2. Rard, J. A., Rand, M. N., Anderegg, G., Wanner, H., Eds.; In *Chemical Thermodynamics 3. Chemical Thermodynamics of Technetium*; Elsevier Science: Lausanne, 1999; p 568.
3. Alberto, R. In *Technetium. Comprehensive Coordination Chemistry-II*; Cleverty, J. M., Meer, T. S., Eds.; Elsevier Science: Amsterdam, 2003; Vol. 4.

4. Dilworth, J. R.; Parrott, S. J. *Chem. Soc. Rev.* **1998**, *27*, 43.
5. Kodina, G. E. In *Isotopes. Properties, Obtaining, Applications*; Baranov, V. Y., Ed.; Atomnaya Energiya: Moscow, 2000.
6. Méndez-Rojas, M. A.; Kharisov, B. I.; Tsivadze, A. Y. *J. Coord. Chem.* **2006**, *59*, 1.
7. Jurisson, S. S.; Lydon, J. D. *Chem. Rev.* **1999**, *99*, 2205.
8. Pauwels, E. K.; Stokkel, M. P. *Q. J. Nucl. Med.* **2001**, *45*, 18.
9. Mark, D.; Bartholom, A.; Louie, S.; John, F. V.; Jon, Z. *Chem. Rev.* **2010**, *110*, 2903.
10. Subramanian, G.; McAfee, J. G.; Blair, R. J.; Kallfelz, F. A.; Thomas, F. D. *J. Nucl. Med.* **1975**, *16*, 744.
11. Bevan, J. A.; Tofe, A. J.; Benedict, J. J.; Francis, M. D.; Barnett, B. L. *J. Nucl. Med.* **1980**, *21*, 961.
12. (a) Lázníček, M.; Lázníčková, A.; Budský, F. *Nucl. Med. Commun.* **1996**, *17*, 1016. (b) Fueger, B. J.; Mitterhauser, M.; Wadsak, W.; Ofluoglu, S.; Traub, T.; Karanikas, G.; Dudczak, R.; Pirich, C. *Nucl. Med. Commun.* **2004**, *25*, 361. (c) El-Mabhouh, A. A.; Angelov, C. A.; Cavell, R.; Mercer, J. R. *Nucl. Med. Biol.* **2006**, *33*, 715. (d) Palma, E.; Oliveira, B. L.; Correia, J. D.; Gano, L.; Maria, L.; Santos, I. C.;Santos, I. *J. Biol. Inorg. Chem.* **2007**, *12*, 667. (e) Asikoglu, M.; Durak, F. G. *Appl. Radiat. Isotopes.* **2009**, *67*, 1616.
13. (a) Guo, X. H.; Luo, S. N.; Wang, H. Y.; Zhou, L.; Xie, M. H.; Ye, W. Z.; Yang, M.; Wang, Y. *Nucl. Sci. Tech*. **2006**, *17*, 285. (b) Yan, X. H.; Luo, S. N.; Niu, G. S.; Ye, W. Z.; Yang, M.; Wang, H. Y.; Xia,Y. M. *Nucl. Sci. Tech*. **2008**, *19*, 165. (c) Chen, C. Q.; Luo, S. N.; Lin, J. G.; Yang, M.; Ye, W. Z.; Qiu, L.; Sang, G. M.; Xia, Y. M. *Nucl. Sci.Tech.* **2009**, *20*, 302. (d) Lin, J. G.; Luo, S. N.; Chen, C. Q.; Qiu, L.; Wang, Y.; Cheng, W.; Ye, W. Z.; Xia, Y. M. *Appl. Radiat. Isotopes* **2010**, *68*, 1616.
14. (a) Libson, K.; Deutsch, E.; Barnett, B. L. *J. Am. Chem. Soc.* **1980**, *102*, 2476. (b) Martin, J. L., Jr.; Yuan, J.; Lunte, C. E.; Elder, R. C.; Heineman, W. R.; Deutsch, E. *Inorg. Chem*. **1989**, *28*, 2899. (c) Elder, R. C.; Yuan, J.; Helmer, B.; Pipes, D.; Deutsch, K.; Deutsch, E. *Inorg. Chem.* **1997**, *36*, 3055. (d) Qiu, L.; Lin, J. G.; Ju, X. H.; Gong, X. D.; Luo, S. N. *Chin. J. Chem. Phys.* **2011**, in press.
15. Koch, W.; Holthausen, M. C. *A Chemist's Guide to Density Functional Theory*; Wiley-VCH: Weinheim, Germany, 2000.
16. Stratmann, R. E.; Scuseria, G. E.; Frisch, M. J. *J. Chem. Phys.* **1998**, *109*, 8218.
17. (a) Becke, A. D. *J. Chem. Phys.* **1993**, *98*, 5648. (b) Lee, C.; Yang, W.; Parr, R. G. *Phys. Rev. B* **1988**, *37*, 785.
18. Hay, P. J.; Wadt, W. R. *J. Chem. Phys.* **1985**, *82*, 299.
19. Hariharan, P. C.; Pople, J. A. *Theor. Chim. Acta* **1973**, *28*, 213.
20. Peterson, K. A.; Figgen, D.; Dolg, M.; Stoll, H. *J. Chem. Phys.* **2007**, *126*, 124101.
21. Godbout, N.; Salahub, D. R.; Andzelm, J.; Wimmer, E. *Can. J. Chem*. **1992**, *70*, 560.
22. Mulliken, R. S. *J. Chem. Phys.* **1955**, *23*, 1833.
23. Foster, J. P.; Weinhold, F. *J. Am. Chem. Soc.* **1980**, *102*, 7211.
24. GaussView, release 3.0; Gaussian Inc.: Pittsburgh, PA, 2003.
25. Tomasi, J.; Mennucci, B.; Cammi, R. *Chem. Rev.* **2005**, *105*, 2999.
26. Frisch, M. J.; Trucks, G. W.; Schlegel, H. B.; Scuseria, G. E.; Robb, M. A.; Cheeseman, J. R.; Montgomery, J. A., Jr.; Vreven, T.; Kudin, K. N.; Burant, J. C.; Millam, J. M.; Iyengar, S. S.; Tomasi, J.; Barone, V.; Mennucci, B.; Cossi, M.; Scalmani, G.; Rega, N.; Petersson, G. A.; Nakatsuji, H.; Hada, M.; Ehara, M.; Toyota, K.; Fukuda, R.; Hasegawa, J.; Ishida, M.; Nakajima, T.; Honda, Y.; Kitao, O.; Nakai, H.; Klene, M.; Li, X.; Knox, J. E.; Hratchian, H. P.; Cross, J. B.; Adamo, C.; Jaramillo, J.; Gomperts, R.; Stratmann, R. E.; Yazyev, O.; Austin, A. J.; Cammi, R.; Pomelli, C.; Ochterski, J. W.; Ayala, P. Y.; Morokuma, K.; Voth, G. A.; Salvador, P.; Dannenberg, J. J.; Zakrzewski, V. G.; Dapprich, S.; Daniels, A. D.; Strain, M. C.; Farkas, O.; Malick, D. K.; Rabuck, A. D.; Raghavachari, K.; Foresman, J. B.; Ortiz, J. V.; Cui, Q.; Baboul, A. G.; Clifford, S.; Cioslowski, J.; Stefanov, B. B.; Liu, G.; Liashenko, A.; Piskorz, P.; Komaromi, I.; Martin, R. L.; Fox, D. J.; Keith, T.; Al-Laham, M. A.; Peng, C. Y.; Nanayakkara, A.; Challacombe, M.; Gill, P. M. W.; Johnson, B.; Chen, W.; Wong, M. W.; Gonzalez, C.; Pople, J. A. *Gaussian 03*, Revision C.02. Wallingford CT: Gaussian, Inc., 2004.
27. Reed, A. E.; Weinstock, R. B.; Weinhold, F. *J. Chem. Phys.* **1985**, *83*, 735.
28. Schäffer, C. E. *Inorg. Chim. Acta* **2000**, *300-302*, 1035.
29. Pauling, L. C. In *The Nature of the Chemical Bond*, 3rd ed.; Cornell University Press: Ithaca, NY, 1960; p 172.
30. (a) Uchtman, V. A.; Gloss, R. A. *J. Phys. Chem.* **1972**, *76*, 1298. (b) Räsänen, J. P.; Pohjala, E.; Nikander, H.; Pakkanen, T. A. *J. Phys. Chem. A* **1997**, *101*, 5196.
31. Reed, A. E.; Curtiss, L. A.; Weinhold, F. *Chem. Rev.* **1988**, *88*, 899.
32. Wiberg, K. A. *Tetrahedron* **1968**, *24*, 1083.
33. (a) Neuhaus, A.; Veldkamp, A.; Frenking, G. *Inorg. Chem.* **1994**, *33*, 5278. (b) Machura, B.; Jaworska, M.; Lodowski, P. *J. Mol. Struc.-Theochem.* **2006**, *766*, 1. (c) Gancheff, J. S.; Albuquerque, R. Q.; Guerrero-Martínez, A.; Pape, T.; De Cola, L.; Hahn, F. E. *Eur. J. Inorg. Chem.* **2009**, 4043.
34. Soloman, E. I., Lever, A. B. P., Eds.; *Inorganic and Electronic Spectroscopy*, *Volume II*, *Applications and Case Studies*; Wiley and Sons Inc.: New York, 1999.
35. (a) Zhang, T. T.; Jia, J. F.; Wu, H. S. *J. Phys. Chem. A* **2010**, *114*, 12251. (b) Fraser, M. G.; Blackman, A. G.; Irwin, G. I. S.; Easton, C. P.; Gordon, K. C. *Inorg. Chem.* **2010**, *49*, 5180. (c) Yoshihide, N.; Ken, S.; Shigeyoshi, S. *Int. J. Quantum Chem.* **2009**, *109*, 2319. (d) Machura, B.; Kusz, J.; Tabak, D.; Kruszynski, R. *Polyhedron.* **2009**, *28*, 493.
36. Liu, C. G.; Su, Z. M.; Guan, W.; Yan, L. K. *Inorg. Chem.* **2009**, *48*, 541.
37. Rodriuez, L.; Ferrer, M.; Rossell, O.; Duarte, F. J. S.; Santos, A. G.; Lima, J. C. *J. Photochem. Photobiol. A: Chem.* **2009**, *204*, 174.
38. Kamlet, M. J.; Taft, R. W. *J. Am. Chem. Soc.* **1976**, *98*, 377.